

Provided for non-commercial research and education use.
Not for reproduction, distribution or commercial use.



This article appeared in a journal published by Elsevier. The attached copy is furnished to the author for internal non-commercial research and education use, including for instruction at the authors institution and sharing with colleagues.

Other uses, including reproduction and distribution, or selling or licensing copies, or posting to personal, institutional or third party websites are prohibited.

In most cases authors are permitted to post their version of the article (e.g. in Word or Tex form) to their personal website or institutional repository. Authors requiring further information regarding Elsevier's archiving and manuscript policies are encouraged to visit:

<http://www.elsevier.com/copyright>



Ionic conductivity of plasma-sprayed nanocrystalline yttria-stabilized zirconia electrolyte for solid oxide fuel cells

Y. Chen,^a S. Omar,^b A.K. Keshri,^a K. Balani,^{a,d} K. Babu,^c J.C. Nino,^b
S. Seal^c and A. Agarwal^{a,*}

^aPlasma Forming Laboratory, Mechanical and Materials Engineering, Florida International University, Miami, FL 33174, USA

^bMaterials Science and Engineering, University of Florida, Gainesville, FL 32611, USA

^cAdvanced Materials Processing & Analysis Center (AMPAC) and Mechanical, Materials and Aerospace Engineering, University of Central Florida, Orlando, FL 32816, USA

^dMaterials and Metallurgical Engineering, Indian Institute of Technology, Kanpur, UP 208016, India

Received 11 February 2009; accepted 22 February 2009

Available online 26 February 2009

Nanocrystalline 10 mol.% yttria-stabilized zirconia (YSZ) electrolyte was synthesized via the plasma spray technique. The ionic conductivity was measured using AC impedance spectroscopy within the temperature range 350–600 °C in air. The measured total ionic conductivity of plasma-sprayed YSZ electrolyte is ~2.3 times higher than that of sintered YSZ electrolyte at 600 °C in air. The improvement in ionic conductivity is ascribed to the nanocrystalline grain size and siliceous free grain boundary with grain-to-grain contact.

© 2009 Acta Materialia Inc. Published by Elsevier Ltd. All rights reserved.

Keywords: Yttria-stabilized zirconia; Electrolyte; Plasma spray; Ionic conductivity

Solid oxide fuel cells (SOFCs) have been attracting attention due to their efficient conversion of electrochemical fuel to electricity with negligible pollution [1–3]. Yttria-stabilized zirconia (YSZ) with a cubic fluorite structure is considered to be the most reliable electrolyte because it exhibits thermal stability, good ionic conductivity at high-temperature (~1000 °C) and thermal expansion compatibility with electrode materials [2–3]. From the view of long-term durability and reliability, and cost efficiency, the current developmental target for SOFCs is to reduce the operating temperature into the intermediate temperature (IT) range (500–700 °C), which requires increased electrolyte ionic conductivity and enhanced gas/electrode reaction kinetics [4]. However, the relatively lower ionic conductivity of YSZ at intermediate temperatures limits its application as an electrolyte candidate for IT-SOFCs.

Nanocrystalline YSZ has a high number of atoms residing at grain boundaries and surfaces that increase the surface area of the active sites for reactions [5]. It is reported that nanocrystalline YSZ exhibits an increase

of about 2–3 orders of the magnitude in electrical conductivity as compared to microcrystalline specimen [4]. Activation energy for microcrystalline YSZ is ~1.24–1.30 eV, whereas this reduces to ~0.93 eV for nanocrystalline YSZ [4]. Therefore, the development of nanocrystalline YSZ electrolyte is of considerable interest for IT-SOFCs. A few researchers have also reported a decrease in the electrical conductivity with decreasing grain size (0.2–20 μm) for zirconia and ceria-based electrolytes [5–10]. These contradictory observations further motivate our present study to understand the effect of grain size on electrical conductivity.

Plasma spray technique is a versatile process: it can deposit almost any material as coatings and bulk while retaining the benefits of rapid solidification, high deposition rate and cost efficiency [9]. Compared with conventional wet ceramic techniques [10] for SOFC electrolyte fabrication, plasma-sprayed materials usually exhibit porous and lamellar microstructures, subsequently leading to low open circuit voltage and cell efficiency. Hence, some post-deposition heat treatments such as high-temperature sintering and spark plasma sintering (SPS) are employed to improve the electrolyte density and alleviate the gas leakage issue [2]. Our research group has successfully synthesized nanocrystalline metal

* Corresponding author. Tel.: +1 305 348 1701; fax: +1 305 348 1932; e-mail: agarwala@fiu.edu

(Al) and ceramic (Al_2O_3) coatings using the plasma spray technique with retention of nanocrystalline structure [11,12]. In the current investigation, nanocrystalline 10 mol.% YSZ electrolyte for IT-SOFCs was synthesized using an atmospheric plasma spray technique. The total ionic conductivity and microstructure of the plasma-sprayed electrolyte was evaluated.

Nanoparticles cannot be directly plasma sprayed, because of their low mass and resultant inability to be carried in a moving gas stream [13]. In addition, they easily clog the plasma gun nozzle due to interparticle friction. Hence, powder treatment such as spray drying becomes essential for consistent powder flow during plasma spraying. Spray-dried nanocrystalline 10 mol.% YSZ powder (Nanox™ 4017, Inframat) with spherical agglomerates 10–50 μm in diameter (Fig. 1a) was selected as the powder feedstock. Each agglomerate consists of fine YSZ particles with a size range of ~ 80 –250 nm, as shown in Figure 1b. Plasma spraying was conducted using a Praxair SG 100 gun on AISI 1020 steel substrate. The plasma spray parameters are listed in Table 1. The YSZ coating (~ 3.5 mm in thickness) was successfully deposited for ionic conductivity experiments. In order to evaluate the ionic conductivity of the plasma-sprayed electrolyte, the 10 mol.% YSZ pellets were also synthesized via conventional solid-state sintering. Spray-dried

10 mol.% YSZ powder was mixed by ball-milling in deionized water with 1% dispersant for 24 h and subsequently dried in the oven at 120 °C for 16 h. The dried powder was then sieved using a 212 μm mesh. Dried powder was uniaxially pressed into disk-shaped pellets (of ~ 8 mm in diameter and ~ 3 mm in thickness) using polyvinyl alcohol (~ 1 wt.%) as a binder under a pressure of 180 MPa. This was followed by the isostatic pressing at 200 MPa for 3 min. Finally, the green ceramic pellets were sintered (solid-state sintering) in air at 1550 °C for 10 h (these pellets are hereafter referred to as sintered YSZ sample).

Microstructure was characterized by field emission scanning electron microscopy (JEOL JSM 6330F) and high-resolution transmission electron microscopy (TEM; Philips CM 200). X-ray diffraction (XRD) patterns were obtained using a diffractometer (Siemens D-500) operating at 40 kV and 20 mA with a $\text{CuK}\alpha$ peak of 1.54 Å. Free-standing plasma-sprayed YSZ sample was obtained by sectioning with low-speed diamond saw. The relative density of the plasma-sprayed and sintered 10 mol.% YSZ samples was first measured geometrically and then using Archimedes' principle. Electrolyte samples were polished to obtain planar surfaces, Pt paste (CL11-5349, Heraeus) was applied to both sides of the free-standing plasma-sprayed samples and sintered pellets to serve as the electrodes. Electrolyte samples were then co-fired at 900 °C for 1 h. Pt wires (99.9% pure) 0.127 mm in diameter were attached to the cell using Pt paste to perform ionic conductivity measurements. The thermocouple was kept in close proximity to the sample to minimize the temperature measurement errors. The complex impedance (Z) measurements of YSZ electrolytes were carried out in air within the temperature range of 350–600 °C using the two-point probe AC impedance spectroscopy technique over a frequency range of 0.10 Hz to 32 MHz. It should be noted that the electronic conductivity of YSZ is negligible [14], and hence the measured electrical conductivity using impedance measurements can be regarded as its ionic conductivity.

Figure 2 shows the XRD patterns of spray-dried 10 mol.% YSZ powders and plasma-sprayed 10 mol.% YSZ electrolyte. Both samples show the presence of a single cubic zirconia phase. No monoclinic or other metastable phases were observed in plasma-sprayed 10 mol.% YSZ. The average density of plasma-sprayed YSZ electrolyte is $\sim 82.7\%$, whereas sintered YSZ electrolyte has a density of $\sim 98\%$ of the theoretical density. Sintered YSZ electrolyte exhibits microcrystalline grains and micron-sized pores (Fig. 3a). The microstructure of the plasma-sprayed 10 mol.% YSZ electrolyte is bimodal in nature, consisting nanocrystalline grains and micron-sized columnar grains (Fig. 3b). Columnar grains exist in fully melted region, whereas nanocrystalline grains are found in partially melted/sintered regions.

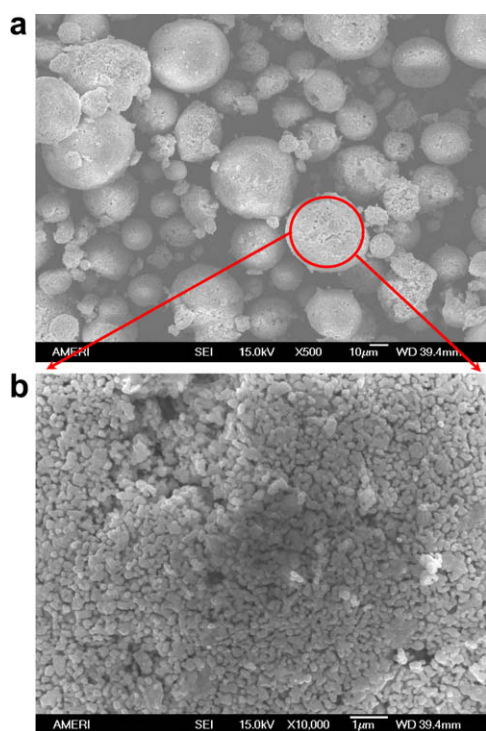


Figure 1. SEM micrographs showing (a) the spray-dried 10 mol.% YSZ spherical agglomerate and (b) a high-magnification view of an agglomerate consisting nanocrystalline particles.

Table 1. Plasma spray processing parameters.

Plasma parameters	Volts (V)	Current (A)	Primary gas, Ar (slm)	Secondary gas, He (slm)	Carrier gas, Ar (slm)	Spray distance (mm)
10 mol.% YSZ coating	40	800	32	60	20	101.6

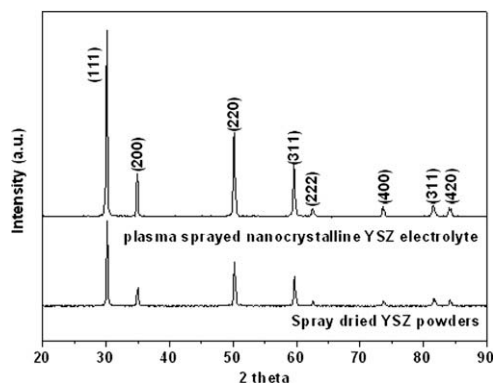


Figure 2. XRD patterns of spray-dried nanocrystalline YSZ powders and plasma-sprayed nanocrystalline YSZ electrolyte.

TEM micrograph (Fig. 3c) of plasma-sprayed YSZ electrolyte shows that the dominant grain size in the partially melted zone ranges is ~ 80 – 150 nm, which is similar to the initial powder size. This implies that partially the melted region did not undergo grain growth during plasma spraying. Direct grain-to-grain contact prevails at the grain boundary which is free from secondary siliceous phase (Fig. 3d). The existence of siliceous phase at the grain boundaries is well known to decrease the grain boundary ionic conductivity [15].

Figure 4a and b shows the Arrhenius plots and actual ionic conductivity, respectively, for plasma-sprayed and sintered YSZ electrolytes. It is clear that the measured total ionic conductivity of plasma-sprayed YSZ is ~ 2.3 times higher than sintered YSZ at 600 °C. Total ionic conductivities of the two samples differ slightly at

350 °C. Correspondingly, Table 2 indicates that activation energy (~ 1.273 eV) for sintered 10 mol.% YSZ is higher than activation energy (~ 1.054 eV) for plasma-sprayed nanocrystalline 10 mol.% YSZ. The pre-exponential factor of sintered 10 mol.% YSZ is higher than that of plasma-sprayed 10 mol.% YSZ, which is consistent with the fact reported by Hui et al. [4]. The activation energy of plasma-sprayed conventional 8 mol.% YSZ is reported to be ~ 1.14 eV in the 600 – 700 °C temperature range [16], which is higher than that of plasma-sprayed nanocrystalline 10 mol.% YSZ. Moreover, it is noteworthy that the measured ionic conductivity, ~ 0.00198 S cm^{-1} , at 600 °C of plasma-sprayed nanocrystalline 10 mol.% YSZ electrolyte is ~ 3.3 times higher as compared to plasma-sprayed microcrystalline 8 mol.% YSZ electrolyte, 0.00059 S cm^{-1} [16]. The above-mentioned results strongly imply that the nanocrystalline structure of YSZ contributes to the improved ionic conductivity.

It is well known that the ionic conductivity of the electrolytes is dominated by the amount of free oxygen vacancies, which is also correlated with the activation energy for oxygen diffusion. As for the YSZ electrolyte, the oxygen vacancies exist mainly in the forms of V_{O}^{\bullet} and $Y'_{\text{Zr}}V_{\text{O}}^{\bullet\bullet}$, in which defects associate ($Y'_{\text{Zr}}V_{\text{O}}^{\bullet\bullet}$) and bind some oxygen vacancies to yttrium ions, leading to the oxygen vacancies being unavailable for conduction. Thermal dissociation of $Y'_{\text{Zr}}V_{\text{O}}^{\bullet\bullet}$ requires extra energy to liberate oxygen vacancies from the defect association, i.e. activation energy actually consists of dissociation energy E_{a} , and migration energy E_{m} . It is noted that the ionic conductivity is directly proportional to the amount of free oxygen vacancy in YSZ electrolytes, which is

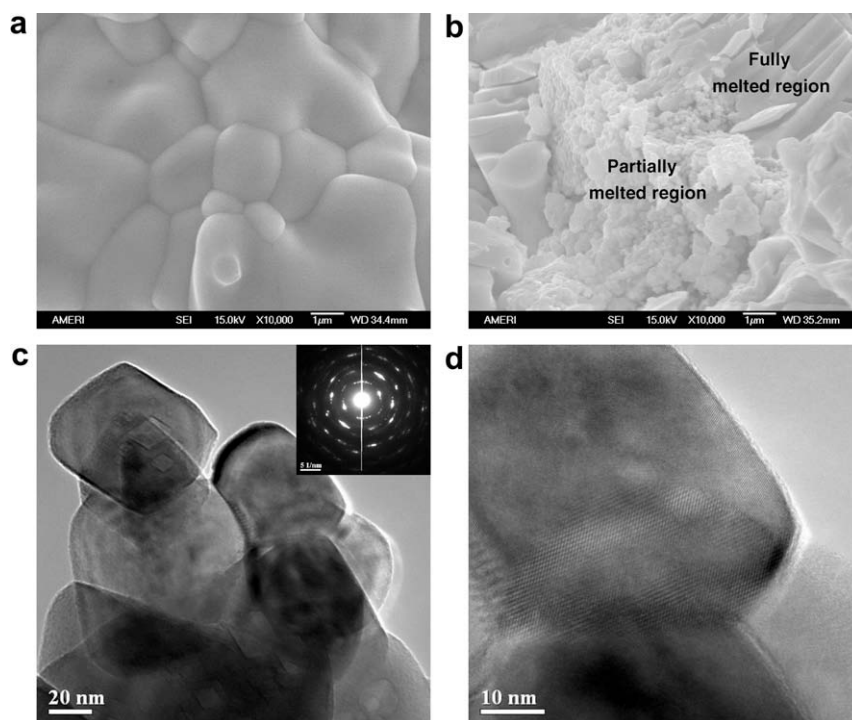


Figure 3. SEM micrographs showing (a) the microstructure of sintered YSZ, (b) the bimodal microstructure of the plasma-sprayed YSZ. TEM micrographs of plasma-sprayed YSZ showing (c) the nanocrystalline YSZ (inset the selected area diffraction patterns of YSZ) and (d) the grain-boundary characteristics.

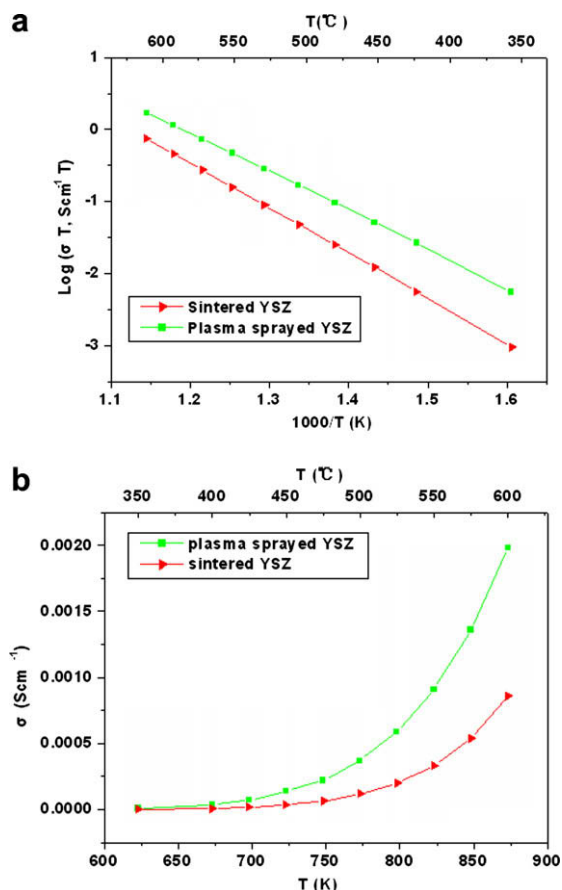


Figure 4. (a) Arrhenius plots for the total ionic conductivity and (b) temperature dependence of ionic conductivity for plasma-sprayed nanocrystalline YSZ electrolyte and sintered YSZ electrolyte, respectively.

Table 2. Comparison of the E_a and σ_0 for plasma-sprayed nanocrystalline YSZ and sintered YSZ electrolytes measured below 600 °C.

Material	E_a (eV)	$\log \sigma_0$
Plasma-sprayed 10 mol.% YSZ	1.054	6.304
Sintered 10 mol.% YSZ	1.273	7.276

strongly determined by its activation energy [17]. Hence, the lower activation energy of the plasma-sprayed nanocrystalline 10 mol.% YSZ causes higher concentration of free oxygen vacancy, which leads to improved grain ionic conductivity (a constituent of total ionic conductivity). Also, in nanocrystalline materials, a large number of atoms (up to 49%) are boundary atoms, which makes conduction properties interface-controlled [4]. Some researchers have ascribed the improved ionic conductivity to spatial modulation of the lattice, quantum confinement of charge carriers, and a dominant contribution from largely defective and strained grain boundaries accompanied with nanocrystalline microstructure [18,19]. In addition, it is commonly accepted that an intergranular siliceous phase significantly de-

grades the ionic conductivity (especially the grain boundary ionic conductivity) of YSZ [15]. Therefore, the lower activation energy in plasma-sprayed 10 mol.% nanocrystalline YSZ and siliceous phase-free grain boundary are hypothesized to be due to the improvement in its ionic conductivity. A comparison with ceria-based electrolytes for IT range suggests that the activation energy of Sm^{3+} and Nd^{3+} co-doped ceria ($\text{Sm}_x\text{Gd}_y\text{Ce}_{1-2x}\text{O}_{2-\delta}$) is low $\sim 0.6867 \pm 0.003$ eV (below 550 °C) [20], indicating higher ionic conductivity than that of plasma-sprayed nanocrystalline YSZ. However, due to the ease of large-scale processing and cost efficiency, plasma-sprayed nanocrystalline 10 mol.% YSZ is a competitive electrolyte candidate for the IT range.

In summary, 10 mol.% YSZ electrolyte synthesized using the atmospheric plasma spray technique exhibited nanocrystalline grain size and siliceous phase-free grain boundaries, imparting improved ionic conductivity in the temperature range 350–600 °C. However, to minimize the loss in voltage due to leaks across the electrolyte, reduction in the porosity through optimization of plasma processing parameters and post-spray heat treatments should be explored in future research.

The authors acknowledge financial support from NASA (Grant No. 16266038-1) to perform this research.

- [1] M.C. Williams, J. Strakey, W. Surdoval, J. Power Sour. 159 (2006) 1241.
- [2] R. Hui, Z.W. Wang, O. Kesler, L. Pose, J. Jankovic, S. Yick, R. Maric, D. Ghosh, J. Power Sour. 170 (2007) 308.
- [3] S.M. Haile, Acta Mater. 51 (2003) 5981.
- [4] S.Q. Hui, J. Roller, S. Yick, X.G. Zhang, C.D. Petit, Y.S. Xie, R. Maric, D. Ghosh, J. Power Sour. 172 (2007) 493.
- [5] H.L. Tuller, Solid State Ionics 131 (2000) 143.
- [6] T. Van Dijk, A.J. Burggaaf, Phys. Status Solid. A 63 (1981) 229.
- [7] S.P.S. badwal, J. Drennan, J. Mater. Sci. 22 (1987) 3231.
- [8] X.J. Chen, K.A. Khor, S.H. Chan, L.G. Yu, Mater. Sci. Eng. A335 (2002) 246.
- [9] P. Fauchais, J. Phys. D 37 (2004) R86.
- [10] J. Will, A. Mitterdorfer, C. Kleinlogel, D. Perednis, L.J. Gauckler, Solid State Ionics 131 (2000) 79.
- [11] A. Agarwal, T. McKechnie, S. Seal, J. Therm. Spray Tech. 12 (2003) 349.
- [12] T. Laha, Arvind Agarwal, T. McKechnie, K. Rea, S. Seal, Acta Mater. 53 (2005) 5429.
- [13] S.O. Chwa, D. Klein, F.L. Toma, G. Bertrand, H. Liao, C. Coddet, A. Ohmori, Surf. Coat. Tech. 194 (2005) 215.
- [14] R.M. Ormerod, Chem. Soc. Rev. 32 (2003) 17.
- [15] X. Guo, R. Waser, Prog. Mater. Sci. 51 (2006) 151.
- [16] C. Zhang, C.J. Li, G. Zhang, X.J. Ning, C.X. Li, H.L. Liao, C. Coddet, Mater. Sci. Eng. 137 B (2007) 24–30.
- [17] E. Iguchi, S. Nakamura, F. Munakata, M. Kurumada, Y. Fujie, J. Appl. Phys. 93 (2003) 3662–3664.
- [18] P. Heitjans, S. Indris, J. Phys. Condens. Matter. 15 (2003) R1257.
- [19] S. Ramasamy, B. Purniah, PINSA 67A (2001) 85.
- [20] S. Omar, E.C. Wachsman, J.C. Nino, Appl. Phys. Lett. 91 (2007) 144106.